

**INTERCALIBRATION OF GEOSTATIONARY (GOES,
METEOSAT, GMS) AND POLAR ORBITING (HIRS, AVHRR,
MODIS) INFRARED WINDOW AND WATER VAPOR RADIANCES**

PURPOSE AND SUMMARY OF DOCUMENT

An overview of the procedures and results for intercalibrating the geostationary infrared window radiances using one polar-orbiting sensor as a reference.

INTERCALIBRATION OF GEOSTATIONARY (GOES, METEOSAT, GMS) AND POLAR ORBITING (HIRS, AVHRR, MODIS) INFRARED WINDOW AND WATER VAPOR RADIANCES

Mathew M. Gunshor (1), Timothy J. Schmit (2), and W. Paul Menzel (2)

1- Cooperative Institute for Meteorological Satellite Studies
2- NOAA/NESDIS/ORA
Madison, Wisconsin 53706 USA

INTRODUCTION

Intercalibration of the polar orbiting and geostationary satellite systems has been started on a routine basis. Monitoring of the consistency of data sets from different sensors has begun. The NESDIS Cooperative Institute for Meteorological Satellite Studies (CIMSS) has been intercalibrating the five geostationary satellites with a single polar orbiting satellite using temporally and spatially co-located measurements. This paper presents the results of over one hundred 11 μm infrared window (IRW) channel comparisons of GOES-8, GOES-10, METEOSAT-5, METEOSAT-7, and GMS-5 with NOAA-14 HIRS and AVHRR. Preliminary results for recently launched instruments, GOES-11 and MODIS, are also presented (both instruments are currently being checked out prior to commissioning). Some comparisons of the 6.7 μm water vapor (WV) channels on GOES-8 and NOAA-14 HIRS are presented as well.

APPROACH

The technique for the intercalibration has been reported in previous CGMS papers; it is repeated here for the sake of completeness. Collocation in space and time (within thirty minutes) is required. Data is selected within 10 degrees from nadir for each instrument in order to minimize viewing angle differences. Measured means of brightness temperatures of similar spectral channels from the two sensors are compared. Data collection is restricted to mostly clear scenes with mean radiances greater than 80 $\text{mW/m}^2/\text{ster/cm}^{-1}$, and no effort is made to screen out clouds from the study area. Data from each satellite is averaged to 100 km resolution to mitigate the effects of different field of view (fov) sizes and sampling densities (HIRS under-samples with a 17.4 km nadir fov, AVHRR GAC achieves 4 km resolution by under-sampling within the fov, MODIS is sampled at 1 km, GOES imager over-samples 4 km in the east west by 1.7, and METEOSAT-5, METEOSAT-7, and GMS-5 have a nadir 5 km fov). Mean radiances are computed within the study area. Clear sky forward calculations (using a global model for estimation of the atmospheric state) are performed to account for differences in the spectral response functions (Figures 1 and 2). The observed radiance difference minus the forward-calculated clear sky radiance difference is then attributed to calibration differences.

Thus

$$\ddot{R}_{\text{cal}} = \ddot{R}_{\text{mean}} - \ddot{R}_{\text{calc}}$$

or for a comparison of a geostationary satellite to HIRS

$$\ddot{R}_{\text{cal}} = [R_{\text{mean}}^{\text{GEO}} - R_{\text{calc}}^{\text{GEO}}] - [R_{\text{mean}}^{\text{HIRS}} - R_{\text{calc}}^{\text{HIRS}}]$$

where GEO indicates geostationary, HIRS indicates the HIRS instrument, mean indicates the mean measured radiance, and calc indicates the forward calculated clear sky radiance. Conversion to temperatures for a comparison between a geostationary satellite to HIRS is accomplished by

$$\ddot{A}T_H = \left[\frac{R_{\text{mean}}^{\text{GEO}}}{dB/dT_{\text{mean}}^{\text{GEO}}} - \frac{R_{\text{calc}}^{\text{GEO}}}{dB/dT_{\text{calc}}^{\text{GEO}}} \right] - \left[\frac{R_{\text{mean}}^{\text{HIRS}}}{dB/dT_{\text{mean}}^{\text{HIRS}}} - \frac{R_{\text{calc}}^{\text{HIRS}}}{dB/dT_{\text{calc}}^{\text{HIRS}}} \right]$$

An identical method is used for calculating the temperature difference between a geostationary satellite and the AVHRR instrument (ΔT_A) and between GOES-8 and MODIS.

RESULTS

Table 1 shows the results for all five geostationary satellites. The absolute mean indicates the mean of the absolute value of all the differences; this is an absolute magnitude of how far from a difference of 0 K each satellite is. The mean indicates the normal mean of all cases and a negative sign indicates HIRS or AVHRR is measuring higher radiances on average than the geostationary instrument. The temperature difference between all geostationary and NOAA-14 instruments is within 0.5 K in the IRW; GOES-8 is within 0.5 K in the WV channel. In nearly all cases the geostationary instruments measure lower radiances, or colder temperatures, than the polar orbiting instruments. This data covers March 1999 through July 2000. No seasonal or diurnal trends have been noticed.

Table 1. March 1999 to July 2000 (May 2000 to July 2000) IRW (WV) comparison of geostationary satellites and NOAA-14 HIRS/AVHRR (HIRS).

Delta (geo – leo)		GOES-8 IRW	GOES-10 IRW	MET-5 IRW	MET-7 IRW	GMS-5 IRW	GOES-8 WV
Number of Comparisons	ΔT_H	20	134	136	153	53	46
	ΔT_A	20	134	136	153	53	-
Absolute Mean	ΔT_H	0.36 K	0.30 K	0.47 K	0.45 K	0.47 K	0.52 K
	ΔT_A	0.22 K	0.14 K	0.41 K	0.33 K	0.42 K	-
Mean	ΔT_H	0.07 K	-0.07 K	-0.37 K	-0.36 K	-0.18K	0.52 K
	ΔT_A	-0.21 K	-0.10 K	-0.39 K	-0.50 K	-0.38 K	-
Standard Deviation	ΔT_H	0.45 K	0.40 K	0.43 K	0.40 K	0.60 K	0.10 K
	ΔT_A	0.13 K	0.17 K	0.27 K	0.32 K	0.30 K	-

AUTOMATION

Computer automated intercalibration has been started in February 2000 and is being reported on the web with daily updates (<http://cimss.ssec.wisc.edu/goes/intercal>). The automated method is about ten times more efficient with no degradation in the intercomparison. Approximately 25% of the cases in Table 1 were processed manually; the remaining 75% were processed without manual intervention. Table 2 shows the percentage of comparisons completed successfully for each geostationary instrument. Cloudy indicates the percentage when the comparison was not attempted because the scene over the comparison region was too cloudy. Failure indicates the percentage when comparison failed due to missing sensor data, missing model data, or other causes. Success rates are not high, however the automated method collects enough data to yield a statistically robust comparison.

Table 2. Efficiency of data comparisons.

Geostationary Satellite	Success (%)	Cloudy (%)	Failure (%)
GOES-8	7	34	59
GOES-10	46	13	41
MET-5	53	10	37
MET-7	53	11	36
GMS-5	19	40	41

NEW SATELLITE INSTRUMENTS

GOES-11 and NOAA-14 IRW channel data have been compared for two cases. The results for the GOES-11 IRW are comparable to those of GOES-8 and GOES-10. For 15 July 2000 at 1045 UTC, mean ΔT_H was -0.01 K and mean ΔT_A was -0.17 K. On 17 July 2000 at 1045 UTC mean ΔT_H was 0.29 K and mean ΔT_A was -0.12 K. For only two cases it is premature to compare these results with those of GOES-8 and GOES-10, though both GOES-11 cases fall well within the range of the other GOES instruments.

Two comparisons of the GOES-8 IRW and WV channel data to that of the polar-orbiting MODIS have also been accomplished. On 30 June 2000 at 1615 UTC and 5 July 2000 at 1635 UTC, GOES-8 IRW and WV was each found to be warmer than MODIS by approximately 0.3 K. MODIS, GOES-8, and NOAA-14 HIRS WV all agree within 0.5 K.

CONCLUSIONS

Five geostationary sensors have been calibrated routinely for over one year with respect to a single polar orbiting sensor. The results, based on between 20 and 153 cases per operational geostationary satellite, suggest the IRW sensors on GOES-8, GOES-10, MET-5, MET-7, and GMS-5 are within 0.5 C of each other (and within 0.5 C of NOAA-14 HIRS and AVHRR). The GOES-8 water vapor sensor is also within approximately 0.5 C of NOAA-14 HIRS. The two cases for GOES-11 and MODIS appear to indicate these two satellites are within the same range of differences. The large number of intercomparisons has enabled early analysis of seasonal and diurnal effects for the first time; none were found. More data must be processed to confirm this. In the future, as more data are being collected, the effect of age on the instruments can be also explored.

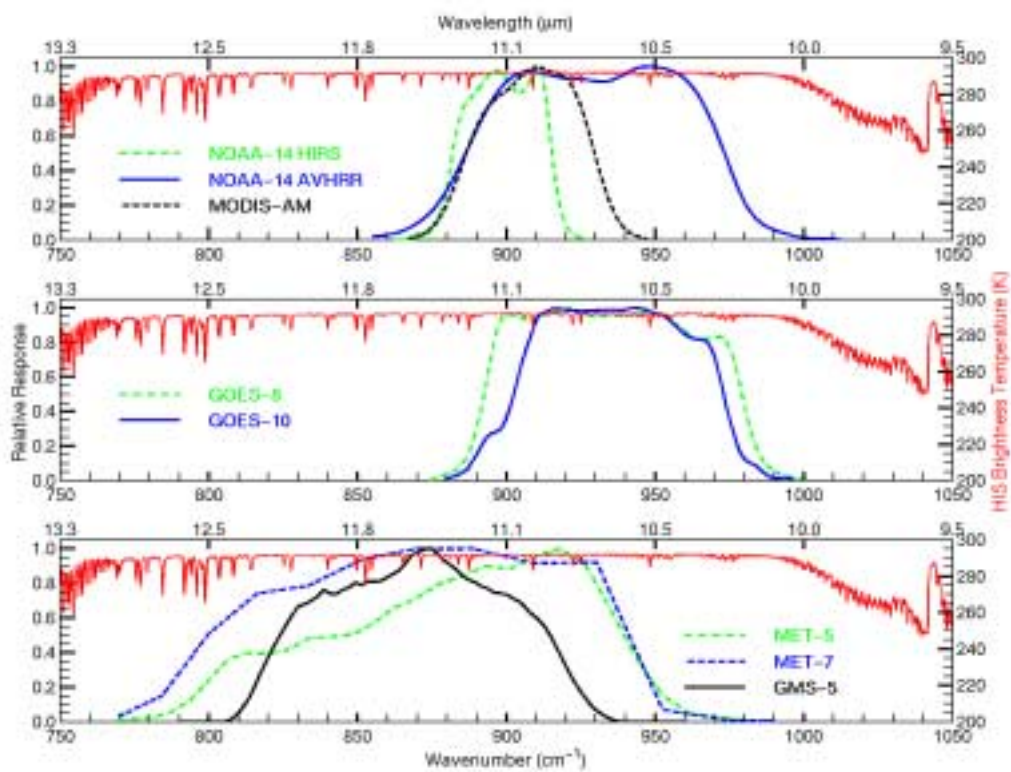


Figure 1. Infrared Window Channel Spectral Response Functions

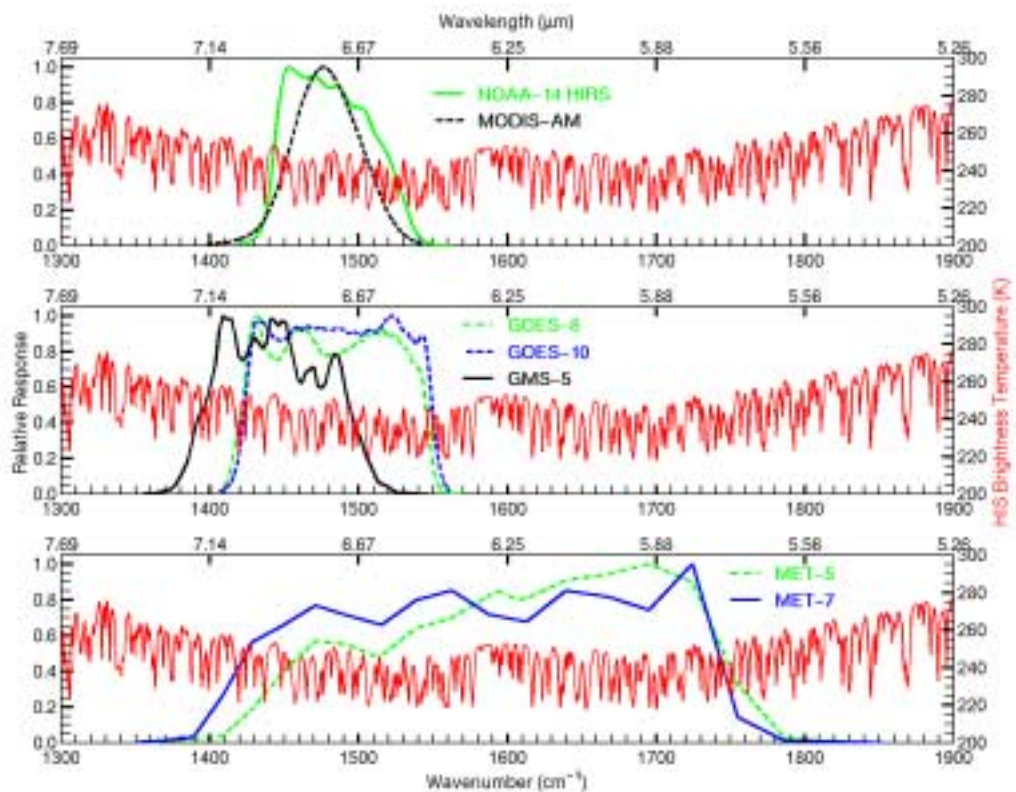


Figure 2. Water vapor channel spectral response functions